

Provided for non-commercial research and education use.
Not for reproduction, distribution or commercial use.



This article appeared in a journal published by Elsevier. The attached copy is furnished to the author for internal non-commercial research and education use, including for instruction at the authors institution and sharing with colleagues.

Other uses, including reproduction and distribution, or selling or licensing copies, or posting to personal, institutional or third party websites are prohibited.

In most cases authors are permitted to post their version of the article (e.g. in Word or Tex form) to their personal website or institutional repository. Authors requiring further information regarding Elsevier's archiving and manuscript policies are encouraged to visit:

<http://www.elsevier.com/copyright>

JMBAvailable online at www.sciencedirect.com

ScienceDirect


Transfer of Flexibility between Ankyrin Repeats in I κ B α upon Formation of the NF- κ B Complex

Shih-Che Sue¹, Carla Cervantes², Elizabeth A. Komives²
and H. Jane Dyson^{1*}

¹Department of Molecular Biology, The Scripps Research Institute, 10550 North Torrey Pines Road, La Jolla, CA 92037, USA

²Department of Chemistry and Biochemistry, University of California, San Diego, 9500 Gilman Drive, La Jolla, CA 92093-0378, USA

Received 10 April 2008;
received in revised form
16 May 2008;
accepted 21 May 2008
Available online
29 May 2008

The mechanism of inhibition of the transcriptional activator nuclear factor κ B (NF- κ B) by the inhibitor I κ B α is central to the understanding of the control of transcriptional activity via this widely employed pathway. Previous studies suggested that I κ B α , a modular protein with an NF- κ B binding domain consisting of six ankyrin repeat domains (ANKs), shows differential flexibility, with ANK 1–4 apparently more rigid in solution in the absence of NF- κ B than ANK 5 and 6. Here we report NMR studies that confirm the enhanced flexibility of ANK 5 and 6 in free I κ B α . Upon binding of NF- κ B, ANK 5 and 6 become well structured and rigid, but, somewhat surprisingly, other domains of the I κ B α , which were relatively rigid in the free protein, become significantly more flexible. Due to the high molecular masses of the component proteins and the complexes, we employ a hierarchical experimental plan to maximize the available information on local flexibility in the ankyrin repeat domains. Backbone resonances of the 221-residue I κ B α protein were assigned firstly in a smaller construct consisting of ankyrin repeats 1–4. These assignments could be readily transferred to the spectra of the construct containing six repeats, both free and complexed with various combinations of the NF- κ B p50 and p65 domains. Transverse relaxation optimized spectroscopy-type NMR experiments on differentially labeled proteins enabled information on backbone structure and dynamics to be obtained, even in complexes with molecular masses approaching 100 kDa. Changes in the flexibility and stability of the various ankyrin repeat domains of I κ B α complex formation take a variety of forms depending on the position of the domain in the complex, providing a variety of examples of the structural and functional utility of intrinsically unstructured or partly folded protein domains.

© 2008 Elsevier Ltd. All rights reserved.

Edited by M. F. Summers

Keywords: NMR relaxation dynamics; hydrogen exchange; TROSY

*Corresponding author. E-mail address:
dyson@scripps.edu.

Abbreviations used: NF- κ B, nuclear factor κ B; ANK, ankyrin repeat domain; NLS, nuclear localization signal; PEST, amino acid composition motif rich in proline (P), glutamic acid (E), serine (S), and threonine (T) residues; MS, mass spectrometry; HSQC, heteronuclear single quantum coherence; TROSY, transverse relaxation optimized spectroscopy; NOE, nuclear Overhauser enhancement; ps–ns, picosecond to nanosecond; PF, protection factor; EDTA, ethylenediaminetetraacetic acid.

Introduction

The nuclear factor κ B (NF- κ B) is the prototype of a family of dimeric eukaryotic transcription factors that is primarily responsible for mediating the expression of many genes by binding to upstream κ B DNA enhancers.^{1,2} In addition, NF- κ B responds to many environmental stimuli, such as bacterial toxins, viruses/viral products and apoptotic/neurotrophic factors. The mammalian NF- κ B family contains five members, p50 (p105), p52 (p100), p65 (RelA), RelB and c-Rel.^{3,4} The heterodimer of p65 and p50 was the earliest form discovered⁵ and represents the most abundant and best-known form of NF- κ B.⁶

In resting cells, NF- κ B is largely sequestered in the cytoplasm in a complex with specific inhibitory proteins of the I κ B family, notably I κ B α . Inhibition and restriction of NF- κ B to the cytoplasm appear to occur through sequestration of nuclear localization signal (NLS) sequences in NF- κ B by tight association with I κ B α .⁶ but I κ B α also appears capable of inhibiting NF- κ B by binding to it at the DNA binding site.⁷

The p50 and p65 subunits of NF- κ B each form two immunoglobulin (Ig)-like domains that together constitute the Rel homology domain of each polypeptide. The N-terminal Ig domain of each subunit makes sequence-specific interactions with the κ B DNA sequence, while the C-terminal Ig domains are involved in DNA backbone contacts, dimerization and binding to members of the I κ B family.⁸ X-ray crystal structures of a number of complexes^{9–11} indicate that the NLS peptide of p65 is masked in the I κ B α complex, but the NLS of p50 remains accessible.¹² In addition, there are accessible nuclear export signals in I κ B α ¹³ and p65,¹⁴ resulting in a dynamic shuttling of the NF- κ B–I κ B α complex between nucleus and cytoplasm, with a preponderance in the cytoplasm.¹² When I κ B α is degraded following an external signal or cellular stress, the balance between nuclear export and import is disturbed: the p65 NLS is now accessible and the I κ B α nuclear export signal has been removed, giving rise to a net increase in the population of NF- κ B in the nucleus.¹⁵

The structure of I κ B α in complex with the p50/p65 heterodimer of NF- κ B^{9,10} includes six ankyrin repeats and a C-terminal PEST sequence. The ANK structural repeat is one of most common structural motifs found in proteins¹⁶ and consists of a β -hairpin followed by two antiparallel α -helices. The PEST is an amino acid composition motif rich in proline (P), glutamic acid (E), serine (S), and threonine (T) residues; it has been reported to be related to protein degradation.^{17,18} I κ B α and NF- κ B form an extensive noncontiguous binding surface in which ANK 1–2 contacts the p65 C-terminal NLS of NF- κ B and ANK 4–6 is closely associated with the dimerization domains of NF- κ B p50 and p65, denoted p50(248–350) and p65(190–289), respectively.

X-ray crystal structures necessarily give a static picture of the inhibitory process mediated by complex formation among proteins. Although I κ B α is well structured in the two crystal structures,^{9,10} no crystals have been obtained for free I κ B α , suggesting that there may be structural and/or dynamic differences in the free protein. Biophysical studies¹⁹ showed that the ankyrin repeat domains of I κ B α are not all well folded in the absence of NF- κ B: in the free protein, the third repeat is the most compact, with repeats 1, 5 and 6 the most solvent accessible, according to amide ¹H/²H exchange experiments.¹⁹ Binding of 1-anilino-8-naphthalene sulfonate and amide exchange indicated that the free protein has considerable molten globule character. An extensive thermodynamic study²⁰

suggested that parts of the component proteins may fold upon complex formation and this was confirmed by amide ¹H/²H exchange mass spectrometry (MS) experiments comparing the exchange of free I κ B α to NF- κ B-bound I κ B α .²¹ In order to elucidate sites of coupled folding and binding as well as to evaluate the role of I κ B α flexibility in its function, we have undertaken an NMR dynamics study of I κ B α and several of its complexes with NF- κ B domains. Since these complexes are large and in some cases consist of several different polypeptide chains, we have evolved a strategy for labeling and overexpression of the components of each complex that enables site-specific structural and dynamic information to be obtained for I κ B α in complexes of increasing size, up to and including the complex with full-length NF- κ B.

Protein segmental disorder and flexibility has been recognized as a common occurrence in regulatory systems in the cell, including signaling, cell cycle, transcriptional and translational control.^{22–25} A number of binding sites in regulatory molecules show intrinsic disorder and fold upon binding to the partner molecule, which may also have a degree of flexibility or disorder. This paradigm allows for great versatility in the binding interactions of regulatory proteins, bestowing the potential for a high level of selectivity arising from the relatively large contact surface, together with reversibility of the interaction arising from the modest affinity and, frequently, efficient regulation by proteolysis. Here we demonstrate that the significant changes that occur in the backbone flexibility of I κ B α when it binds to NF- κ B provide a complete program of reciprocal mobility changes that serve to allow the inhibitor to perform each of its functions with exquisite specificity.

Results

Design and differential labeling of I κ B α and NF- κ B constructs

I κ B α consists of a 317-residue polypeptide containing phosphorylation sites in the N- and C-terminal sections (related to the degradation of the inhibitor), and six ankyrin (ANK) repeat domains that function as the binding site for NF- κ B. The minimal fragment required for binding and dissociation of DNA-bound NF- κ B contains residues K67 to E287 [I κ B α (67–287)],^{7,26} encompassing the entire six ANK repeats and the first seven residues of C-terminal PEST sequence (Fig. 1).

The p50 subunit used in this study contains the dimerization [p50(248–350)] and N-terminal DNA-binding [p50(39–247)] domains, whereas the p65 construct further contains a NLS sequence at C-terminus in addition to residues 19–321 of p65. A streamlined preparation of heterodimers of p50(248–350)/p65(190–321) and p50(39–350)/p65(19–321) exclusive of homodimer contamination is described in the Supplementary Material. Complexes

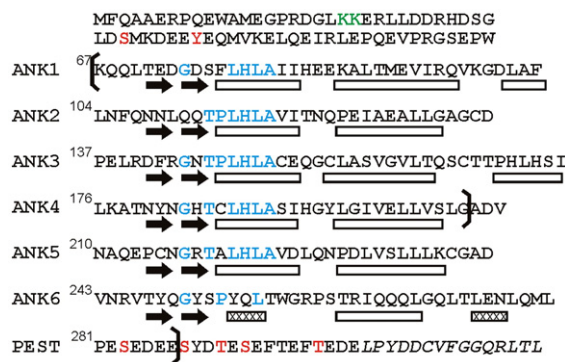


Fig. 1. Amino acid sequence of human I κ B α showing the positions of the ankyrin repeats and the PEST domain. Positions of secondary-structure elements in the X-ray crystal structure of I κ B α in complex with p50(19–321)/p50(248–350)¹⁰ are indicated below the sequence. The positions of the hairpin structures in each repeat are indicated by black arrows, and the helices by rectangles, with $_3$ helices shown hatched. Residues that correspond to the ankyrin repeat consensus are shown in blue. Phosphorylation sites are indicated in red, and a ubiquitination site in green. The boundaries of the constructs used in this study (67–287, 67–206) are shown by brackets. The C-terminal sequence thought to be involved in ubiquitin-independent proteasome degradation²⁷ is shown in italics.

of I κ B α (67–287) (labeled with ^{13}C , ^{15}N and ^2H) with highly deuterated heterodimers of p50/p65 were prepared using a variation of this method.

Backbone assignment strategy

To obtain site-specific information on the dynamics of I κ B α free and bound to NF- κ B, it is necessary to obtain as complete a set of site-specific resonance assignments as possible. There are several challenges: firstly, the large molecular size of the complex, total 94 kDa [24.3 kDa I κ B α and 69.5 kDa p50(39–350)/p65(19–321) heterodimer]; secondly, the similarity of structure and consensus sequence in the ANK repeats; and thirdly, broadened and missing resonances, shown by the mismatch between residue number and peak number in ^1H - ^{15}N heteronuclear single quantum coherence (HSQC) or ^1H - ^{15}N transverse relaxation optimized spectroscopy (TROSY)-HSQC spectra. The first difficulty can be overcome by adopting TROSY-type pulse schemes combined with highly deuterated samples. The second and third problems result in severe ambiguities in the assignments between the various ANK repeat domains. The problems are particularly severe if the 94-kDa p50/p65 complexed I κ B α (67–287) is targeted directly. Instead, we use a different approach that utilizes assignments made on the free domains or on truncated versions. The assignments can be transferred to larger proteins and complexes if the fragments share structural similarity.^{28,29}

Resonance broadening and absence are particularly severe for free I κ B α (67–287), as illustrated in Fig. 2a (black spectrum). To minimize weak associa-

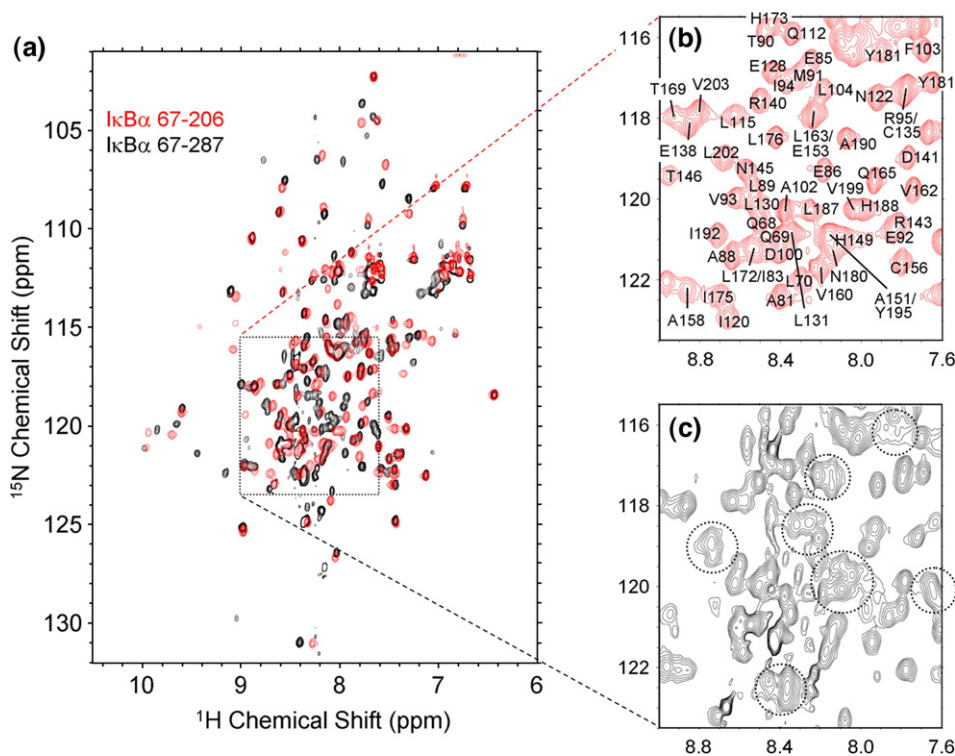


Fig. 2. (a) Superposition of the ^1H - ^{15}N HSQC of [^2H , ^{15}N , ^{13}C]-I κ B α (67–286) (black) and [^2H , ^{15}N , ^{13}C]-I κ B α (67–206) (red), showing the overall correspondence between the two spectra. (b) Expanded region of the spectrum of I κ B α (67–206) showing assignments. (c) The same expanded region of the spectrum of I κ B α (67–287) showing broadened resonances, indicated by dotted circles.

tion, all NMR data were acquired at 0.1 mM and 20 °C. The black spectrum in Fig. 2a shows that a portion of the molecule is well structured, resulting in widely dispersed cross peaks of uniform size. These cross peaks correspond to the residues in ANK 1–4, as illustrated by the close correspondence of the positions of these peaks with those seen in the HSQC spectrum of a shorter construct, I κ B α (67–206), representing ANK 1–4 (superimposed in red in Fig. 2a). These resonances could be uniquely assigned, as illustrated in Fig. 2b, but the superposition in Fig. 2a shows that there are not enough additional peaks in the black spectrum to account for the expected resonances of ANK 5 and 6 in I κ B α (67–287). At lower contour levels, a number of weak and broadened resonances appear between ^1H chemical shift 7.6 and 9.0 ppm, as indicated by dotted circles in Fig. 2c. These cross peaks occur in the central “random coil” region of the spectrum, indicating that a significant part of free I κ B α (67–287) is unfolded and/or in conformational exchange.

Given the potential difficulties associated with the conformational heterogeneity of ANK 5–6 in the free protein, we utilize a strategy to obtain resonance assignments for bound I κ B α that involves NMR analysis of a number of truncated fragments and complexes: (i) free I κ B α (67–206), (ii) I κ B α (67–206) in

complex with p65 NLS (residues 289–321), (iii) I κ B α (67–287) in complex with p50(248–350)/p65 (190–321), (iv) I κ B α (67–206) in complex with p65 (19–321)/p50(248–350) (analogous to the domains that are seen in the X-ray crystal structure) and finally, (v) I κ B α (67–287) in complex with p65(19–321)/p50(39–350). The proteins and complexes (i)–(iii) have lower molecular weights than the target complexes (iv) and (v), resulting in better coherence transfer in three-dimensional (3-D) triple-resonance spectra; resonance assignments made by these means for the smaller proteins and complexes can be readily transferred to the (extensively deuterated) larger one by analysis of simple TROSY-based ^{15}N and triple-resonance spectra. A schematic illustration of this assignment strategy is shown in Fig. 3 for I κ B α fragments that are ^2H , ^{13}C , ^{15}N labeled, either free or in complex with extensively ^2H labeled NF- κB elements.

Backbone resonances of (i) free I κ B α (67–206) were assigned using conventional 3-D HNCA, HN(CO)CA, HNCACB and HN(CO)CACB spectra.³¹ Some of the resonances near the N-terminus of the β -hairpin of ANK 1 show broadening and low intensity; the ^1H - ^{15}N cross peak of S159 is missing in the HSQC spectrum. Missing cross peaks are summarized for all complexes in Table 1.

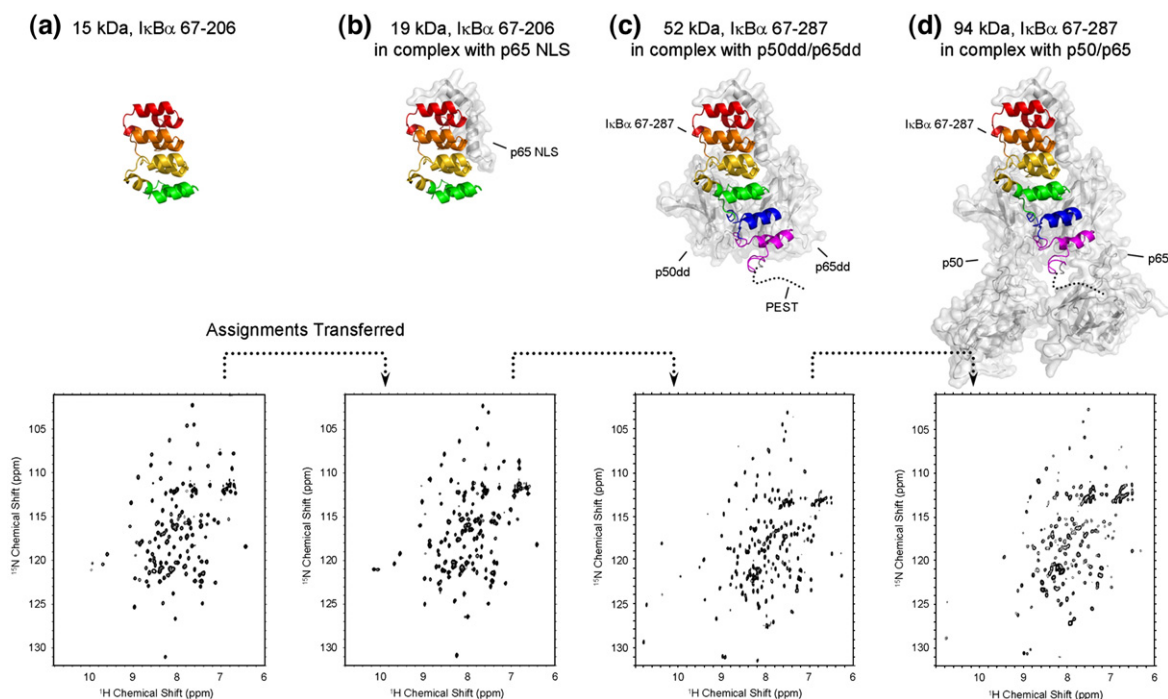


Fig. 3. Schematic diagram showing the assignment strategy for the 94-kDa complex of p50(39–350)/p65(19–321) with I κ B α (67–287) based on transfer of assignments from smaller proteins and complexes. The top row shows putative structures of the complexes, modeled from X-ray crystal structures (Jacobs and Harrison¹⁰ for a, b, c and d and Chen *et al.*³⁰ for d). The approximate position of the flexible PEST sequence is indicated by a dotted line. Ankyrin repeats are colored red (ANK 1), orange (ANK 2), yellow (ANK 3), green (ANK 4), blue (ANK 5) and purple (ANK 6). The bottom row shows the 600-MHz ^1H - ^{15}N HSQC spectra (a and b) or 900-MHz TROSY-type HSQCs (c and d) for each I κ B α fragment. (a) [^2H , ^{15}N , ^{13}C]-labeled I κ B α (67–206) (15 kDa), (b) [^2H , ^{15}N , ^{13}C]-I κ B α (67–206) in complex with p65 NLS (residues 289–321 of human p65) (19 kDa), (c) [^2H , ^{15}N , ^{13}C]-I κ B α (67–287) in complex with p50(248–350)/p65(190–321) (52 kDa), (d) [^2H , ^{15}N , ^{13}C]-I κ B α (67–287) in complex with p50(39–350)/p65(19–321). The experimental conditions are 0.5 mM, 20 °C, 600 MHz in (a) and (b), 0.5 mM, 25 °C, 900 MHz in (c) and 0.1 mM, 30 °C, 900 MHz in (d), respectively. The I κ B α fragments are ^{15}N , ^{13}C labeled and highly deuterated; p50 and p65 fragments are deuterated only.

Table 1. Missing residues in individual fragments/complexes

Fragment/Complex	Missing residues in HSQC or TROSY-HSQC spectra
(i) I κ B α (67–206)	S159 (3) ^a
(ii) I κ B α (67–206) in complex with p65 NLS	E72 (1), S159 (3)
(iii) I κ B α (67–287) in complex with p50(248–350)/p65(190–321)	T71 (1), E72 (1), I120 (2), R143 (3), G144 (3), T146 (3), Q154 (3), C156 (3), A158 (3), S159 (3), T168 (3), G197 (4), G259 (5), T263 (5)
(iv) I κ B α (67–287) in complex with p50(248–350)/p65(19–321)	Same as (iii)
(v) I κ B α (67–287) in complex with p50(39–350)/p65(19–321)	Same as (iii), plus weaker peaks broadened at molecular mass 94 kDa: T113 (2), T121 (2), T164 (3), C186 (4), C215 (5), N216 (5), A220 (5)

^a Numbers in parentheses indicate the ANK repeat numbers.

In (ii), the complex of I κ B α (67–206) with the peptide representing the p65 NLS, the residues in ANK 3 and 4 retain similar chemical shifts, but significant perturbations were observed for the ANK 1 and 2 repeats. For transfer of assignments between free I κ B α (67–206) and the NLS complex, the assignments were confirmed using HNCA/HN(CO)CA spectra. Because of the repetitive nature of the I κ B α (67–206) sequence and structure (Fig. 1), the 2-D HSQC and 3-D triple-resonance spectra of the free protein (i) contain a number of ambiguities due to signal overlap. Some assignments for the free protein were actually made by comparison with those of the complex (ii); for example, the cross

peaks of L78 and I83 overlap with those of L189 and L172, respectively, in free I κ B α (67–206), but could be confidently assigned in the I κ B α (67–206)/NLS complex, since these particular overlaps were resolved. The resonances of ANK 1 that are missing or of low intensity in the free I κ B α (67–206) remain the same in the I κ B α (67–206)/NLS complex, and the ¹H–¹⁵N cross peak of one additional residue, E72, cannot be observed because of the attenuated signal.

Since the cross peaks corresponding to ANK 5 and 6 of the free I κ B α (67–287) are not readily observable or distinguishable in the spectra of the free protein (Fig. 2), these resonances were assigned in (iii), the complex of I κ B α (67–287) with p50(248–350)/p65(190–321). This 52-kDa complex can be treated in two sections: ANK 1–3 bound to the p65 NLS (assignment described in the previous paragraph) and ANK 4–6 bound to p50(248–350)/p65(190–289) of NF- κ B. The backbone resonances of ANK 1–3 of (ii), I κ B α (67–206)/NLS, are readily mapped to the corresponding region of (iii), the I κ B α (67–287)/p50(248–350)/p65(190–321) complex; an additional set of TROSY-type triple-resonance experiments, including HNCA/HN(CO)CA and HN(CA)CB/HN(COCA)CB experiments,³² was acquired to confirm the assignments and assign the resonances of ANK 4–6. As commonly observed in large protein systems, the HN(CA)CB and HN(COCA)CB experiments did not show satisfactory intensities for sequential assignments to be made independently, especially for the sequential ¹³C β . However, with the aid of the previous assignments made for significant portions of the protein, together with the relatively complete sequential connectivities available for ¹³C α , assignments could be successfully completed for the complex, and all backbone resonances in the ¹H–¹⁵N TROSY-HSQC spectrum were assigned without ambiguity (Fig. 4). Resolution of ambiguities between ANK repeats is illustrated in Fig. 5, which

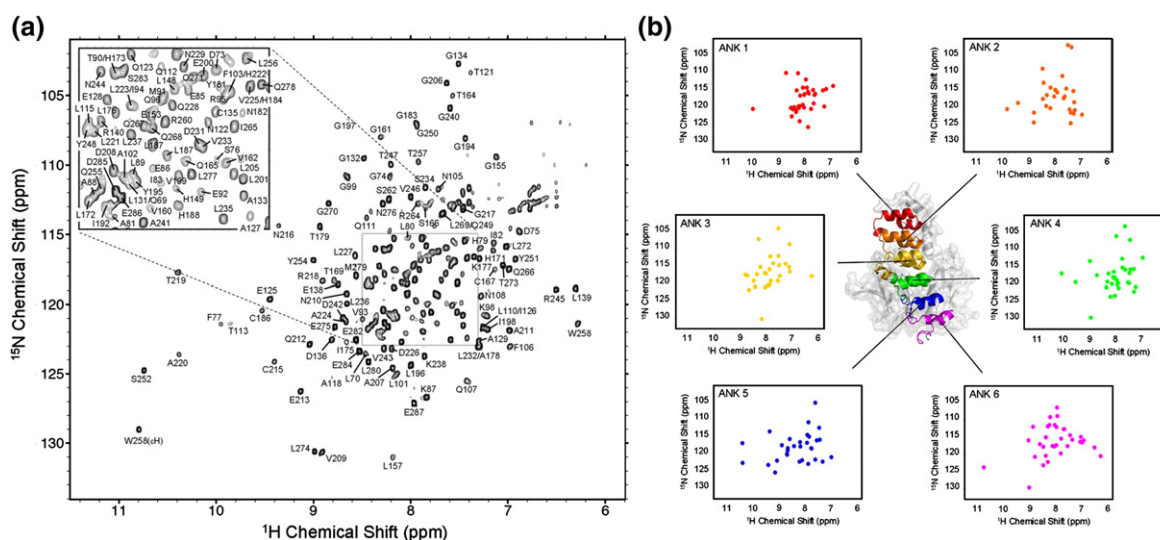


Fig. 4. (a) ¹H–¹⁵N TROSY-HSQC spectrum (900 MHz) of [²H, ¹⁵N, ¹³C]-I κ B α (67–287) in complex with [²H]-p50(248–350)/p65(190–321), recorded at 30 °C. Assignments of the backbone amide resonances are labeled. (b) Distribution of the backbone amides of each ANK repeat plotted separately. Note the relatively small number of amides in the spectrum of ANK 3.

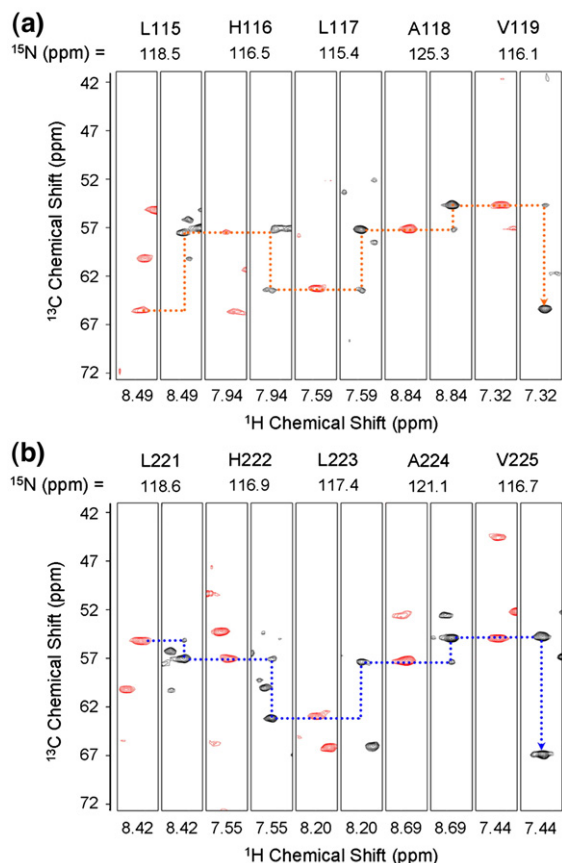


Fig. 5. HNCA (black) and HN(CO)CA (red) strips for two sequences, from 3-D ^1H - ^{15}N TROSY-HNCA (900 MHz) and TROSY-HN(CO)CA (600 MHz) of (^2H , ^{15}N , ^{13}C)-labeled I κ B α (67–287) in complex with ^2H -labeled p50(248–350)/p65(190–321) at 25 °C. $^{13}\text{C}^\alpha$ connectivities (dashed lines) are shown for the identical sequence LHLAV for (a) residues 115–119 (ANK 2) and (b) 221–225 (ANK 5).

shows strips taken from 3-D ^1H , ^{15}N TROSY-HNCA and HNCOCA spectra at the ^{15}N chemical shifts of residues 115–119 (ANK 2) and 221–225 (ANK 5), which have the same amino acid sequence, LHLAV. Despite the identical sequences, the resonances from each of these regions can be unambiguously connected via $^{13}\text{C}^\alpha$ chemical shifts, even when sequential $^{13}\text{C}^\beta$ shifts are of low intensity, as mentioned above.

It is noticeable that a large number of residues in ANK 3 cannot be observed in the ^1H - ^{15}N TROSY-HSQC spectrum, and many other residues in ANK 3 show weaker peak intensities, but with similar chemical shifts as found in the I κ B α (67–206)/NLS complex. These results indicate that the structure of ANK 3 is similar in the free protein and in the complex, but there has been a change in the behavior of all or part of the backbone of ANK 3 in the complex with p50(248–350)/p65(190–321), resulting in broadening of resonances. This is most commonly attributed to the presence of exchange processes on an intermediate (approximately millisecond) time scale. Thus, we observe a change in the dynamics of ANK 3 towards greater structural heterogeneity upon formation of the complex with p50(248–350)/p65(190–321).

For the two larger complexes (iv) I κ B α (67–287) with p50(248–350)/p65(19–321) and (v) I κ B α (67–287) with p50(39–350)/p65(19–321), the peak positions in 2-D TROSY-HSQC spectra are very similar to those seen for (iii) I κ B α (67–287) with p50(248–350)/p65(190–321). An overlay of the TROSY-HSQC spectra of (iii) I κ B α (67–287) with p50(248–350)/p65(190–321) and (v) I κ B α (67–287) with p50(39–350)/p65(19–321) is shown in Fig. S1 of the Supplementary Material. These results indicate that, consistent with the X-ray crystal structures,^{9,10} the presence of the N-terminal domain(s) of NF- κ B barely influences the I κ B α structure or binding interface. Thus, after establishing the assignments of (iii), I κ B α (67–287) in complex with p50(248–350)/p65(190–321), the results could be readily transferred to the 71- (iv) and 94-kDa (v) complexes. The assignments for these two complexes were confirmed by a TROSY-HNCA spectrum of (iv), I κ B α (67–287) in complex with p50(248–350)/p65(19–321).

Secondary structure of I κ B α

Comparison of the observed ^{13}C chemical shifts with the corresponding sequence-corrected random coil values³³ was used to obtain information on the secondary structure present in the free and bound I κ B α . Due to the resonance broadening and overlap, the information for ANK 5 and 6 of the free protein is fragmentary and is not included in the analysis. As a measure of the α or β conformation of the backbone at each residue, we use a parameter, $(\Delta\text{C}^\alpha - \Delta\text{C}^\beta)$, corresponding to the difference between the secondary chemical shifts ΔC^α and ΔC^β , after correcting for deuterium isotope effects.^{34,35} Values of $(\Delta\text{C}^\alpha - \Delta\text{C}^\beta)$ for ANK 1–4 of the free protein and for ANK 1–6 in the I κ B α (67–287)/p50(248–350)/p65(190–321) complex were plotted as a function of residue number (Fig. 6). Positive values indicating α -helix correspond well with those observed in the X-ray crystal structure, indicated at the top of Fig. 6. Correspondence of the negative values, reflecting the locations of β -strands, is less definitive. In particular, the β -strands are not defined in ANK 1 in the complex due to the absence of resonances for L70, T71 and E72. No preference for secondary structure is indicated for the C-terminal PEST sequence, consistent with its likely random-coil character. For free I κ B α (67–206), most peaks are of near-equal intensity, consistent with the overall structural stability of free ANK 1–4. The derived profile of $(\Delta\text{C}^\alpha - \Delta\text{C}^\beta)$ is similar for ANK 1–4 in free I κ B α (67–206) and bound I κ B α (67–287), indicating that there is no significant secondary structural change in the first four repeats when in complex with NF- κ B.

NMR relaxation measurements

Measurement of ^{15}N - R_1 and ^{15}N - R_2 relaxation parameters and the ^1H - ^{15}N heteronuclear nuclear Overhauser enhancement (NOE) gives information primarily on the picosecond to nanosecond (ps–ns) motions of the polypeptide backbone in the free and

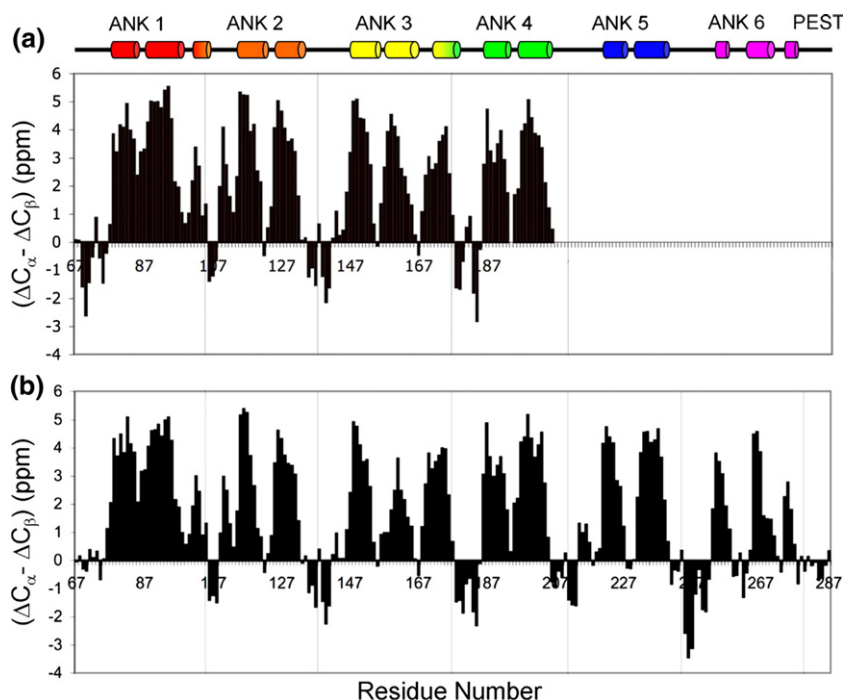


Fig. 6. (a) Secondary structure, evaluated by the parameter $(\Delta C^\alpha - \Delta C^\beta)$ plotted *versus* residue number. I κ B α (67–206). The chemical shift values of $^{13}\text{C}^\alpha$ and $^{13}\text{C}^\beta$ were obtained for free (^{13}C , ^{15}N)-labeled I κ B α (67–206). (b) I κ B α (67–287) in complex with p50(248–350)/p65(190–321). The chemical shift values of $^{13}\text{C}^\alpha$ and $^{13}\text{C}^\beta$ were obtained for the complex of (^2H , ^{13}C , ^{15}N)-labeled I κ B α (67–287) with highly deuterated p50(248–350)/p65(190–321). ΔC^α and ΔC^β were calculated from the difference between the experimental $^{13}\text{C}^\alpha$ and $^{13}\text{C}^\beta$ chemical shifts and the corresponding random coil values. The value of $(\Delta C^\alpha - \Delta C^\beta)$ for each residue represents the average of three consecutive residues, centered at the particular residue.³⁴ The α -helices determined by X-ray for the complex are indicated at the top for comparison.

bound states. The results are plotted in Fig. 7 for I κ B α (67–287) in (iii), the I κ B α (67–287)/p50(248–350)/p65(190–321) complex (black circles) and free I κ B α (67–206) (red circles). The truncated variant I κ B α (67–206) was used instead of I κ B α (67–287) because of difficulties assigning the partially folded regions of the longer construct. In addition, the broadened resonances in the center of the spectrum and the strong resonances of the PEST sequence adversely affected the quantitative measurement of nearby resonances.

I κ B α (67–206) shows very limited conformational flexibility, consistent with the overall stability of this fragment. Similarly, in the I κ B α (67–287)/p50(248–350)/p65(190–321) complex, most of the backbone amides show limited conformational flexibility. The plots for R_1 and R_2 differ significantly between the free I κ B α (67–206) and the I κ B α (67–287)/p50(248–350)/p65(190–321) complex, as expected from the difference in their molecular weights, but the heteronuclear NOE values are almost identical for ANK 1–4, indicating that the backbone of this region of the protein undergoes similar local ps–ns motions whether free or in complex with NF- κ B. The heteronuclear NOE (Fig. 7c) is usually >0.80 , as expected for well-structured proteins, but several regions show greater flexibility. Regions centered around residues 69, 99 and 167 of both free and bound proteins and residue 271 of the bound protein have NOE values <0.6 , indicating flexibility on the ps–ns time scale. In addition, residues 69 and 169 show elevated R_1 (Fig. 7a) and lowered R_2 (Fig. 7b) values, suggesting the presence of motion on a microsecond to millisecond time scale. Apart from the N-terminal region around residue 69, the more flexible residues are thus located in linker regions between ANK repeats. For both free I κ B α (67–206) and bound I κ B α (67–287), the R_2/R_1 ratio, which gives a mea-

sure of the molecular tumbling rate, is similar for residues throughout the molecule, indicating that the ankyrin repeat domains are attached to each other and not tumbling independently. Such behavior is typical of most ankyrin repeat domains¹⁶; the behavior of ANK 5 and 6 in free I κ B α is anomalous. For the PEST sequence, the NOE values gradually approach zero and eventually become negative at the last residue, consistent with the presence of random-coil backbone conformations as inferred from the chemical shift measurements (Fig. 6).

It is noticeable that the entire length of I κ B α in the I κ B α (67–287)/p50(248–350)/p65(190–321) complex shows similar values for R_1 , R_2 and NOE. Greater heterogeneity in the amplitude of T_2 was observed for ANK 1 and 3 and for the N-terminal half of ANK 4: resonances in these regions are of significantly lower intensity than for the rest of the sequence, as reflected in significant error bars. Significant values were not obtained for a number of other low-intensity resonances in this region, which are omitted from the figure. In addition, since other residues in these regions are undetectable, the relaxation information, especially for ANK 3, is incomplete. Interestingly, the detectable residues in ANK 3 do not have above-average T_2 values; we therefore conclude that the phenomenon causing the broadening or loss of resonances in this region occurs on a time scale different from the microsecond to millisecond time scale where the exchange factor R_{ex} can be measured.

NMR hydrogen–deuterium exchange measurements

Detection of hydrogen–deuterium (H/D) exchange in NMR experiments provides direct site-specific information on the rate of exchange of amide protons for deuterium, which can be directly correlated with

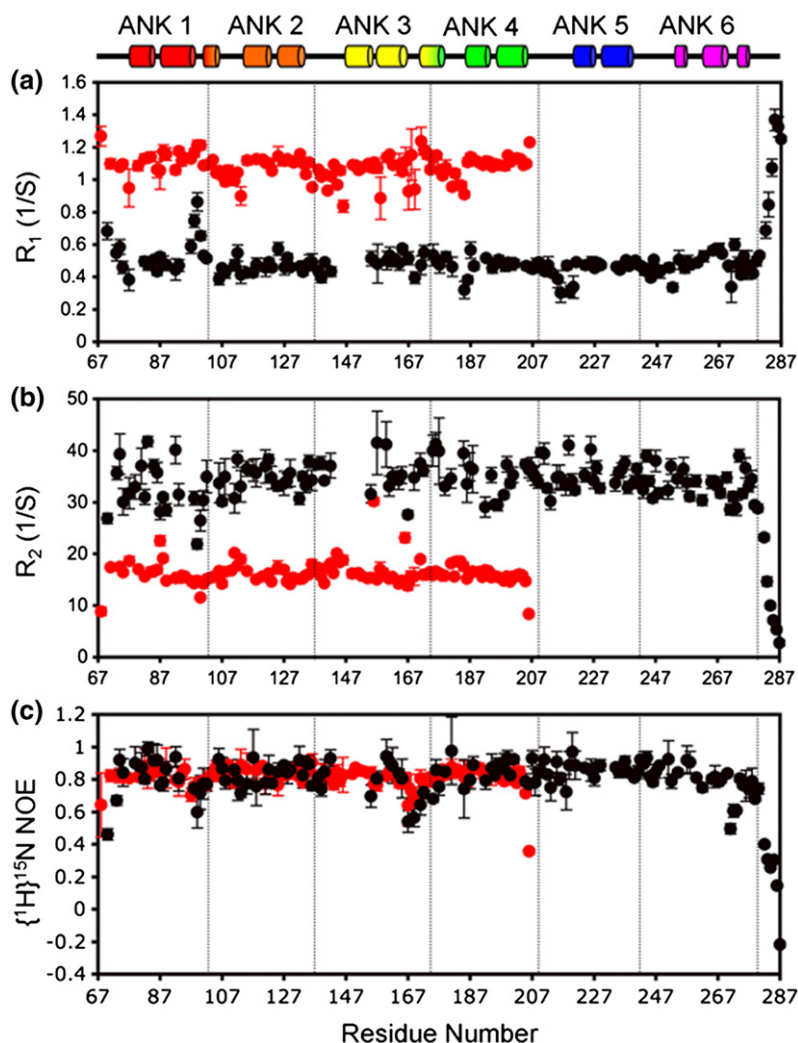


Fig. 7. Backbone amide ^{15}N relaxation rates for I κ B α (67–206) at 20 °C (red circles) and I κ B α (67–287) in complex with p50(248–350)/p65(190–321) at 30 °C (black circles). (a) R_1 , (b) R_2 , (c) ^1H - ^{15}N NOE. The relaxation parameters were measured at 600 MHz. Secondary structure is shown at the top for comparison.

local flexibility of the polypeptide backbone.³⁶ H/D exchange was initiated for two I κ B α samples, free I κ B α (67–206) and the I κ B α (67–287)/p50(248–350)/p65(190–321) complex, by rapid solvent exchange into D $_2$ O at physiological pH. Series of HSQC spectra for free I κ B α (67–206) and TROSY-type HSQC spectra for I κ B α (67–287)/p50(248–350)/p65(190–321) were acquired at increasing intervals after solvent exchange (sample curves of peak intensity *versus* time are given in Supplementary Fig. S6). The protection factor (PF) was calculated at each site by dividing the intrinsic exchange rate k_{int} by the experimentally determined exchange rate k_{ex} .³⁷ The results are plotted in Fig. 8a, and the locations of the persistent amides in free and bound I κ B α are shown in Fig. 8b and c, respectively. Amides whose signals persist in the HSQC or TROSY spectrum after 30, 100 and 1000 min after solvent exchange into D $_2$ O are shown by colored spheres of diameter corresponding to the intensity of the cross peak.

For free I κ B α (67–206), the individual repeats show consistent PF in the four ANKs, in the range of 10^4 to 10^6 . Small areas, such as the β -fingers in ANK 1 and 4 and the variable loops between ANK 1–2 and 3–4 exhibit lower protection, consistent with the presence of dynamic local fluctuations. If the two α -

helices in each repeat are treated as representing a cooperatively folded fragment, we can calculate average PFs to give a comparison of the relative stabilities of individual ANK repeats. The average PFs are 2.2×10^4 for ANK 1, 2.7×10^5 for ANK 2, 8.9×10^4 for ANK 3 and 1.1×10^4 for ANK 4. Although there is decreased protection at the ends, the degree of difference among the four repeats is not dramatic. We conclude that there is no significant dynamic difference between ANK 1–4. The lower PF found in ANK 1 and 4 are likely conferred by higher solvent accessibility and the lack of protection associated with their position on the ends of this construct. For the center of this molecule, consisting of residues 114–154 and including the two ANK 2 helices and the first helix of ANK 3, the average PF is 3.8×10^5 .

The PF of the core reflects the stability of the protein towards unfolding processes that result in solvent exchange; that is, it represents the energy difference (ΔG_{ex}) between the native state and a globally unfolded state. The free energy of H/D exchange ΔG_{ex} is estimated by the relationship $\Delta G_{\text{ex}} = RT \ln(\text{PF})$.³⁸ For the average core PF (stated above as 3.8×10^5) the calculated ΔG_{ex} is 7.5 kcal/mol. If we consider the measured highest observed

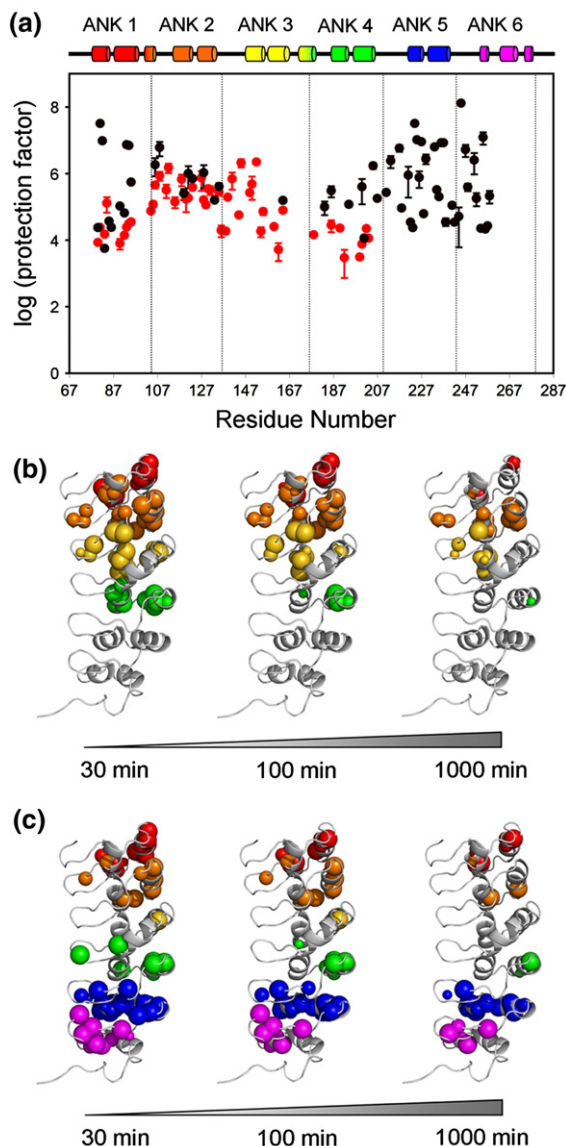


Fig. 8. Protection factors of I κ B α . (a) Profiles show the PFs of backbone amides of I κ B α (67–206) (red) and I κ B α (67–287) in complex with p50(248–350)/p65(190–321) (black). PF values were not determined for residues 82, 96, 119 and 148 of free I κ B α (67–206) or for residues 84, 91, 96, 129, 178, 202, 232, 239 of I κ B α (67–287) in complex with p50(248–350)/p65(190–321) because of resonance overlap. PF values for residues 81, 82, 93, 94, 224, 225, 227, 233 and 236 of I κ B α (67–287) in complex with p50(248–350)/p65(190–321) represent a lower limit since resonance intensities decay slowly within the experiment time. The experimental exchange rates (k_{ex}) for these residues are assumed to be 10^{-5} min^{-1} and standard errors are not available. (b and c) The amides still present in the HSQC spectrum after various H/D exchange time points (30, 100 and 1000 min) are mapped as spheres onto the published structure of I κ B α in the complex.¹⁰ (b) I κ B α (67–206), (c) I κ B α (67–287) in complex with p50(248–350)/p65(190–321). The radius of each sphere reflects the intensity of the cross peak that remains in the HSQC or TROSY-HSQC spectrum. Experiments were recorded at 20 °C, 600 MHz for I κ B α (67–206) and 25 °C, 900 MHz for I κ B α (67–287) in complex with p50(248–350)/p65(190–321).

PF, 2×10^6 , the ΔG_{ex} is ~ 8.4 kcal/mol. These values are close to the reported free energy ΔG_{H_2O} , 6.7 and 7.7 kcal/mol, determined by chemical denaturants urea and guanidinium chloride, respectively.³⁹ Therefore, according to the Linderström–Lang model,⁴⁰ the behavior of ANK 1–4 is in the EX2 limit, indicating that the relative rate of protein closing (k_{cl}) is much faster than the intrinsic proton exchange rate (k_{int}). The consistency between these results reveals the thermodynamic stability for the ANK 1–4 fragment and confirms the highly cooperative unfolding transition reported previously.³⁹

The results for I κ B α (67–287)/p50(248–350)/p65(190–321) show significant differences in the stability of individual repeats compared with the free protein. Firstly, while ANK 5/6 residues are missing or broadened in free I κ B α (67–287), they show consistently high PFs in the complex (Fig. 8a and c). Indeed, the region between the N-terminal end of ANK 5 and the first helix of ANK 6 undergoes the slowest amide exchange of the entire I κ B α . The PFs are generally in the range of 10^6 to 10^8 , generally higher than those of the free protein. The second helix of ANK 6 has higher local flexibility such that no amides can be observed during the experiment. The fingers close to the NF- κ B interface also show high protection, indicating their critical role in binding. The binding of NF- κ B appears to stabilize ANK 5/6 from an incompletely folded or fluxional state in the free protein into an extremely stable structure.

Enhanced protection in ANK 1 and 4 was observed. For ANK 1, this can be explained by the presence of the tightly bound p65 NLS, although ANK 1 remains at the N-terminus of the protein construct that was studied. The role of the bound NLS in stabilizing ANK 1 and 2 can be inferred from a comparison of the two X-ray crystal structures of the NF- κ B–I κ B α complex: in one,¹⁰ the p65 NLS is present and forms a pair of helices bound to ANK 1 and 2, which show well-defined secondary-structure elements. By contrast, in the second structure,⁹ the p65 NLS is absent, the secondary-structure elements of ANK 1 are not well defined and several portions of the polypeptide could not be traced. For ANK 4, several factors are operative. It is no longer at the C-terminus of the protein construct and is now present in the middle of the molecule and stably bound to the p50/p65 heterodimer. ANK 4 should thus be protected both by the proximity of ANK 5 and 6 and by complex formation with NF- κ B.

Somewhat surprisingly, the binding of NF- κ B appears to destabilize the middle repeat, ANK 3: residues in this repeat have significantly lower protection than the corresponding residues in free state. A majority of the amides in ANK 3 cannot be detected even in the first NMR spectrum taken immediately after solvent exchange into D₂O, as indicated in the left panel of Fig. 8c. These results suggest the presence of local backbone fluctuation, mainly limited to the middle of the molecule. Consistent with this, there is a large number of invisible or attenuated resonances in the TROSY-HSQC spectrum of ANK 3 (Fig. 4b). Never-

theless, ANK 3 appears to retain native-like secondary structure in the complex (Fig. 6). These results appear to indicate the presence of fluctuating tertiary structure with intermediate time-scale motion in ANK 3 and the motion consequently broadens the resonances and reduces the backbone stability. Such a change in ankyrin repeat domain dynamics upon complex formation has not been previously reported.

A similar H/D exchange study has been reported using MS of peptide fragments to detect exchange.²¹ A comparison of the results obtained by MS and NMR is shown in Table 2: the number of NMR resonances appearing in the first HSQC spectrum are counted according to the peptide fragment definition.²¹ For free I κ B α , the results obtained by the two methods are mostly very similar, although the NMR results (earliest possible time point 30 min after D₂O solvent exchange) were obtained with the shorter ANK 1–4 fragment [I κ B α (67–206)] and the MS results (time point, 2 min after D₂O solvent exchange), with ANK 1–6 [I κ B α (67–287)]. All of the H/D exchange results are consistent with the presence of modular structure in free I κ B α , with a well-folded domain accompanied by a flexible region. The largest discrepancy between the two sets of PFs is found in the sequence 177–187, the ANK 4 β -finger, where the NMR values are significantly lower, probably due to its presence close to the C-terminus of I κ B α (67–206): the absence of ANK 5 and 6 might reduce the local protection and/or destabilize the local structural packing.

For the complex, there is a significant disagreement in the middle region of the molecule (ANK 3

and 4) between the NMR and MS measurements of residual unexchanged protons. The 2-min mass measurements showed that ANK 3–4 retained protection comparable to that of the remainder of the protein, while the initial (30 min) NMR measurements showed that these protons were largely unprotected. These results show that a significant number of amides remain detectable in ANK 3/4 when the exchange time is shorter than 5 min (exchange rates of 10⁰–10⁻¹ min⁻¹, with PF range 10²–10³ and intrinsic exchange rates close to 10² min⁻¹ under these conditions), but are exchanged within 30 min, the first available time point in the NMR experiment. For example, the residue with exchange rate 10⁻¹ min⁻¹ would still have 82% intensity after 2-min D₂O exchange, but only 5% would remain in the NMR experiment after 30-min D₂O exchange. On the basis of these two results, we estimate that the PFs for amides in this region of the protein are in the range 10²–10³, compared to the values of >10⁴ for the rest of the protein (Fig. 8a). In summary, the data agree very well for the bound I κ B α in repeats 4/5 and 6, which fold upon binding, but do not agree for repeat 3, which did not exchange much in the MS experiment (2-min time point) and did exchange in the NMR experiment (30-min time point). This would be consistent with amides that exchange on an intermediate time scale, as are often found in regions of a protein undergoing conformational fluctuations on the millisecond time scale. This discrepancy thus reflects exactly the time scale of motions that would result in broadened and missing peaks, as we indeed observe for repeat 3 in the NMR experiments.

Table 2. Comparison of H/D exchange monitored by MS and NMR measurements

Region	I κ B α peptides ^a	Total amides	No. of amides ^b			
			Free		Bound	
			MS (after 2 min) ^a	NMR (after 30 min) [I κ B α (67–206)]	MS (after 2 min)	NMR (after 30 min)
ANK 1	66–80	14	2.0	1	4.9	1
	79–91	12	5.6	6	–	9
	92–103	11	4.0	5	3.6	5
ANK 2	104–117	12	9.8	7	9.4	2
	105–117	11	8.6	6	8.0	2
ANK 3	137–150	12	10.5	8	10.6	1
	140–150	9	7.4	6	7.4	1
	142–150	7	6.1	5	5.8	1
	158–176	17	7.3	4	6.9	1
ANK 4	177–187	10	6.2	1	7.0	3
	188–197	9	4.8	5	6.4	1
	188–201	13	8.3	7	8.2	4
ANK 4/5	201–220	18	3.9	4 [201–206] ^c	12.3	9
	201–223	20	2.7	4 [201–206] ^c	13.3	12
	202–223	19	2.3	3 [202–206] ^c	12.7	11
ANK 6	242–257	14	0	–	10.9	11
	243–257	13	0	–	10.6	10
	258–272	13	0	–	1.3	1
	258–274	15	0	–	2.0	1

^a Modified from Table 1 of the paper by Truhlar *et al.*²¹

^b Number of amides that remain unexchanged, calculated from the mass increase at the 2-min time point²¹ or from cross peaks remaining in the NMR spectrum at the earliest time point.

^c Construct ends at residue 206.

Discussion

Missing resonances as a measure of backbone motion

The major problem in the interpretation of the NMR spectrum of the free six-ANK protein I κ B α (67–287) is the broadening or absence of a number of resonances in ANK 5 and 6. This observation can be taken as a signal of motion within the polypeptide on an intermediate (approximately microsecond) time scale and can be used in conjunction with the H/D exchange data and the relaxation data for the observable NMR resonances to map changes in the motional characteristics of the polypeptide chain in the free and complexed I κ B α (67–287). The nature of the conformational heterogeneity in ANK 5 and 6 in the free protein is indicated by a comparison of secondary and tertiary structural parameters between the various repeats. CD spectra¹⁹ suggest that similar secondary structures are present in the free and bound states. The fluctuations that cause broadening and disappearance of resonances in the spectra of ANK 5 and 6 must therefore be large-scale fluctuations of secondary-structure elements, perhaps between a “folded” state that resembles the bound structure and an “unfolded” state where the secondary-structure elements are not connected in a coherent ankyrin-type fold. Since such a large-scale structure change would be relatively slow and would also result in major differences in chemical shift between the resonances of a given residue in the two different states, it is reasonable that the resulting exchange broadening might render the resonances invisible. A similar mechanism has been invoked to explain the absence of resonances belonging to the F helix of apomyoglobin.⁴¹

New and different resonances go missing upon complex formation with NF- κ B. In addition to residues where the ¹H–¹⁵N cross peak of HSQC or TROSY–HSQC spectra is missing, a lesser degree of motional broadening can also be inferred from the 3-D triple-resonance data. Strikingly, a significant fraction of I κ B α ¹³C $^{\alpha}$ and ¹³C $^{\beta}$ resonances is missing for (iii), the complex of I κ B α (67–287) with p50(248–350)/p65(190–321), particularly in the ANK 1 β -hairpin and ANK 3, while the resonances of ANK 5 and 6 are virtually all present, indicating the formation of a well-structured complex with p65(190–321)/p50(248–350). Both the present NMR experiments and our previous ¹H/²H experiments²¹ showed that ANK 5 and 6 appear to fold upon binding, although binding was not accompanied by an increased helical CD signal.¹⁹ Similarly, the “unfolded” character of ANK 3 in the complex most likely consists mainly of increased dynamics and not of loss of secondary structure, since this is still present in the crystal structures.^{9,10}

NF- κ B/I κ B α are examples of “incompletely folded functional proteins”

It appears that unfolded and partly folded proteins may not only be functional, but their relative

lack of structural stability may be required for their function.^{25,42} One of the tenets of this hypothesis is that the folded state of a polypeptide and the dynamics of the backbone and side chains change in the presence of partners. The NF- κ B/I κ B α system provides a variety of illustrations of this principle through the variety of foldedness and flexibility that occurs in the free and bound proteins. This is illustrated schematically in Fig. 9. The structure of I κ B α in the p50/p65 complex¹⁰ can be divided into four regions according to the dynamic behavior observed (presence or absence of NMR resonances, amide proton PFs and relaxation behavior).

Region 1 consists of ANK 1 and 2. Apart from the N-terminus of ANK 1, this segment of the protein is well structured in both the free state and bound to p50(248–350)/p65(190–321). This is shown firstly by the uniform intensity of the resonances of these two repeats within the NMR spectrum of each of the free protein constructs and in all of the complexes as well as by the uniform values of the relaxation parameters (Fig. 7) and the generally high PFs (Fig. 8). This part of the protein makes contact with the p65 NLS in the X-ray structure.¹⁰ NMR experiments on a peptide representing the NLS alone (C. Cervantes and E. A. Komives, unpublished data) show that this sequence is unfolded in the free state and becomes folded when bound to

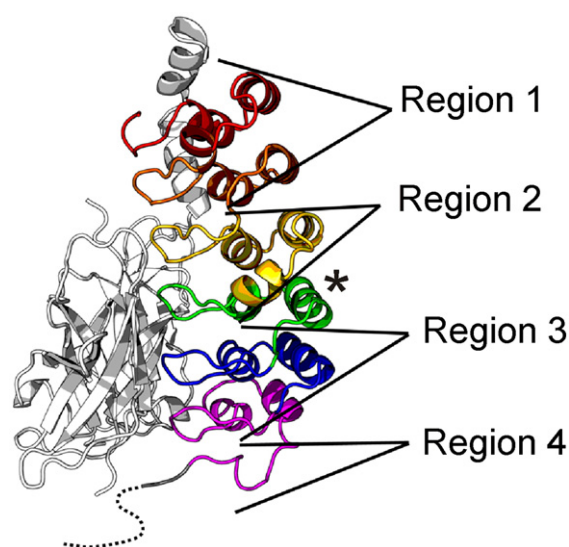


Fig. 9. Regions of I κ B α that vary in their dynamic characteristics in the free and bound states, mapped onto the X-ray structure of the I κ B α (67–287)/NF- κ B complex.¹⁰ Ankyrin repeats are colored as in Fig. 3. Regions are defined according to their flexibility and solvent accessibility, as judged by H/D exchange, relaxation parameters and presence of unbroadened resonances (see the text). For Region 1, average free PF, $\sim 10^4$ – 10^6 , and average bound PF, $\sim 10^4$ – 10^8 ; for Region 2, average free PF, $\sim 10^4$ – 10^6 , and average bound PF, $\sim 10^2$ – 10^3 ; for Region 3, average free PF, $\sim 10^0$ – 10^1 , and average bound PF, $\sim 10^4$ – 10^8 ; for Region 4, average free PF, $\sim 10^0$ – 10^1 , and average bound PF, $\sim 10^0$ – 10^1 . The C-terminal helix of ANK 4 (asterisk) is protected in both free and complexed I κ B α and has therefore been excluded from Regions 3 and 4.

I κ B α (67–206). Thus, the relatively well structured Region 1 of I κ B α forms a structured scaffold for the coupled folding and binding of the unstructured p65 NLS and remains relatively rigid whether free or bound to p50/p65.

Region 2 consists of ANK 3 and the N-terminal helix of ANK 4. This portion of the protein appears to undergo an unusual transition upon binding of p50/p65: from a relatively well structured and rigid domain to a fluxional structure, for which a number of resonances are missing from the NMR spectrum and which appears to be more flexible than the free form of the protein, as shown by the PFs (Fig. 8). The absence of many of the resonances in ANK 3 and the broadness of the remaining resonances argue for a relatively slow time-scale process of exchange between (at least) two conformers with significantly different NMR spectra. The usual explanation for the absence of cross peaks such as we see here is that the molecule is in “intermediate exchange,” neither fast exchange (where a cross peak would appear at the point representing a population-weighted average of the chemical shifts in the ensemble) nor slow exchange (where cross peaks would appear in two separate positions). Intermediate exchange, resulting in broadening of the resonances, sometimes to invisibility, occurs when the rate of exchange is in between fast and slow and the chemical shift difference between the states is appropriate. Further broadening of the cross peaks will also occur because of the greater size of the complex compared to the free protein. However, since the remainder of the resonances in I κ B α are visible for the complex, we conclude that the difference for Region 2 arises due to motion. Although we cannot make quantitative statements on the rates of exchange in this instance, we can definitively state that the absent cross peaks represent motion in the backbone that was not present in the free protein.

Region 3 consists of ANK 5 and 6. This region shows less motion in the complex compared to the free protein. Indeed, most of the resonances of ANK 5 and 6 are absent or broadened in the spectrum of I κ B α (67–287). We infer from the absence of these resonances that ANK 5 and 6 undergo motion on an intermediate time scale in the free protein. In the complex, these motions are damped out, and Region 3 appears to be the most stable part of the protein, as shown by PFs (Fig. 8). The heteronuclear NOE values (Fig. 7c) clearly show that this part of the protein is as rigid on the ps–ns time scale as the rest of the protein. It appears that we are observing in this region a classic folding and structure stabilization upon binding transition. The flexibility of ANK 5 and 6 in the free state is apparently necessary for function: mutation of residues in these two repeats to render their sequences closer to the consensus ankyrin repeat sequence has succeeded in increasing the stability of ANK 5 and 6 to the point where the cross peaks belonging to this region of the protein are visible in the NMR spectrum (data not shown), but the mutant protein is found to be impaired in function. The process of degradation of

free I κ B α by a proteasome-dependent but ubiquitin-independent mechanism is slower for the prefolded mutants, and these mutants bind NF- κ B more weakly due to a faster dissociation rate (k_{off}).⁴³ We conclude that the relative instability and incomplete folding of ANK 5 and 6 in I κ B α is functionally important, possibly because an incompletely ordered structure would facilitate rapid proteolytic degradation and/or would allow greater freedom to form a stable complex with a large surface area of contact, as is found for other unstructured proteins that fold upon binding to partners.^{25,44} Certainly, it appears likely that the inability of free ANK 1–6 to form diffraction-quality crystals for X-ray analysis (G. Ghosh, personal communication) may be related to the relatively heterogeneous ensemble of structures indicated for ANK 5 and 6 in the free state.

Region 4 consists of the PEST sequence. This region remains unstructured in both the free and complexed forms of I κ B α , and strong NMR resonances are observed, indicating that the motions of this sequence are uncoupled to the motions of the protein or complex as a whole. The PEST sequence (Fig. 1) was truncated in the construct used for NMR, consistent with the best-defined residues in the X-ray structures.^{9,10} The PEST fragment that we included in our construct was well-structured in the crystal structure of the complex, and its position, in contact with the DNA-binding domain of p65, prompted the hypothesis that the PEST sequence was directly involved with removal of NF- κ B from DNA through complex formation and neutralization of basic DNA-binding residues.⁹ We see no evidence for the tight binding of the PEST sequence to the remainder of the complex, even in I κ B α (67–287)/p50(39–350)/p65(19–321), indicated by the presence of sharp NMR signals belonging to the PEST sequence residues in positions very little changed from those of the free protein (data not shown). We are continuing to investigate this question, as the truncation of the PEST sequence in our construct may have destabilized the interaction.

Static and dynamic picture of the complex

X-ray data give a static picture of molecular structure, but the distribution of *B*-factor values can be used to give information on local mobility in the context of the crystal. The *B*-factors in the two X-ray structures of NF- κ B–I κ B α ^{9,10} show low values (indicating better structural accuracy) for ANK 4–6 in complex with p50(248–350)/p65(190–321) and significantly higher values for ANK 1–2 in complex with the NLS. The NLS sequence itself shows the highest *B*-factor values in the entire complex, consistent with its presence as an unstructured domain in the free NF- κ B and as a single-helical motif in the complex. Comparing this result with the NMR dynamics measurements, where ANK 1 and 2 are also highly structured, we infer that the apparent motion in the crystal, evidenced by the *B*-factors of the NLS

and the ANK 1–2 region, may in fact indicate that the motion we observe in ANK 3 is giving rise to a wobbling motion that results in segmental flexibility of the two ends of the complex. Thus, we observe in the NMR experiments fluctuation in the interface at ANK 3, which appears in the crystal as though ANK 1–2 and the NLS are fluctuating. We conclude that the X-ray data are consistent with the presence of segmental motion pivoted at ANK 3 in I κ B α after binding to NF- κ B.

Transfer of flexibility between ankyrin repeats upon complex formation

Because many of the cross peaks are broadened or absent, NMR methods cannot give quantitative estimates of the dynamics of ANK 5 and 6 in the free I κ B α . However, it is clear that there is considerable flexibility in this region, and it is equally clear that it becomes highly structured, rigid and resistant to amide proton exchange upon complexation with NF- κ B. Such a disorder-to-order transition should involve a considerable loss of conformational entropy in ANK 5 and 6. By contrast, ANK 1 and 2 are relatively rigid in the free state and serve as a template to bind the p65 NLS, which is intrinsically unstructured in the free NF- κ B. Again, the process of complex formation should result in a considerable loss of conformational entropy as the NLS folds into a helical structure upon binding I κ B α . In between these two regions is ANK 3, which paradoxically appears to become more flexible in the complex than in the free protein. The flexibility inherent in the NLS and in ANK 5 and 6 has apparently been transferred to ANK 3. There may be several reasons for this. Firstly, ANK 3 may have a lower contact surface on NF- κ B, since it is between the NLS (binding to ANK 1 and 2) and the main body of the p50 and p65 dimerization domains (binding to ANK 5 and 6). However, the transfer of flexibility from one part of the molecule may also help to compensate for the loss of conformational entropy upon complex formation. When NF- κ B binds I κ B α , the overall binding energy is mainly contributed by a favorable ΔH (–15 kcal/mol) and a surprisingly small unfavorable $-T\Delta S$ (+1.9 kcal/mol).⁴³ Truncation and mutation experiments have shown that the thermodynamic hotspots of the interaction are at the ends of the complex; deletion of helix 4 (residues 305–321) of p65 decreases binding by 8000-fold²⁰ and a similar effect is seen upon deletion of the C-terminus (residues 275–317) of I κ B α (S. Bergqvist and E. Komives, unpublished data). In addition, mutation of interface residues in the third repeat based on the crystal structure had little or no effect on binding.⁴⁵ These results taken together with the NMR experiments presented here raise the possibility that NF- κ B/I κ B α complex formation, incorporating relatively tight binding of the ends of the elongated interface, causes a slight dissociation and disordering of ANK 3 that can be visualized as a “squeezing” of the ends of the complex.

Materials and Methods

Expression and purification of proteins

General preparation and purification methods for I κ B α (67–287) have been described previously,^{19,39} and I κ B α (67–206) was prepared and purified in the same way. Expression of [²H, ¹³C, ¹⁵N]-labeled I κ B α (67–287) or I κ B α (67–206) was carried out in M9 minimal medium in D₂O supplemented with ¹⁵NH₄Cl (0.5 g/L), ¹⁵NH₄SO₄ (1 g/L) and ¹³C-labeled glucose (2 g/L). The culture was induced by 0.1 mM IPTG at 15 °C with 24-h incubation. Cells were resuspended with lysis buffer [50 mM phosphate buffer (pH 8.0)/150 mM NaCl/10 mM imidazole] and lysed by sonication.

A pure heterodimer of NF- κ B p50/p65 was prepared using a variation of the published method.⁴⁶ A streamlined method for the production of I κ B α complexes of pure heterodimer uncontaminated by p50/p50 or p65/p65 homodimers is described in the Supplementary Material. In this method, the incorporation of a hexahistidine tag on the N-terminus of the p65 construct to be expressed allows rapid purification of both pure heterodimers [p50(248–350)/p65(190–321) or p50(39–350)/p65(19–321)] or of differentially labeled complexes with I κ B α (67–287). The desired complex is efficiently separated using a single nickel-affinity column with a subsequent gel-filtration column. The p50 (39–350) and p50(248–350) fragments represent residues 39–350 and 248–350, respectively, and p65(19–321) and p65 (190–321) fragments represent residues 19–321 and 190–321, respectively.

NMR backbone triple-resonance experiments

Resonance assignments for I κ B α free and in complex with NF- κ B were made using triply labeled [²H, ¹³C, ¹⁵N] I κ B α . For most samples, HNCA,^{31,47} HN(CO)CA,^{31,47} HN(CA)CB,^{31,48} HN(COCA)CB³¹ and HNCO⁴⁷ spectra, or their TROSY equivalents³² were acquired.

For triply labeled [²H, ¹³C, ¹⁵N] I κ B α (67–206), NMR spectra were acquired at 20 °C on a Bruker DRX600 spectrometer equipped with a cryoprobe. The sample was exchanged for NMR into the following buffer: 25 mM Tris (pH 7.5)/50 mM NaCl/50 mM arginine/50 mM glutamic acid/5 mM Chaps/1 mM ethylenediaminetetraacetic acid (EDTA)/1 mM DTT in 90% H₂O and 10% D₂O. The following parameters were used in the 3-D experiments: for HNCA, data size=2048 (t3)×48 (t2)×96 (t1) complex points, number of scans=8; for HN(CO)CA, data size=2048 (t3)×40 (t2)×96 (t1) complex points, number of scans=16; for HN(CA)CB, data size=1024 (t3)×32 (t2)×90 (t1) complex points, number of scans=32; for HN(COCA)CB, data size=1024 (t3)×32 (t2)×90 (t1) complex points, number of scans=40; for HNCO, data size=2048 (t3)×48 (t2)×96 (t1) complex points, number of scans=4. The delay time between each scan is 1.5 s.

For the complex between triply labeled [²H, ¹³C, ¹⁵N] I κ B α (67–206) and the p65 NLS peptide, NMR spectra were acquired at 20 °C on a Bruker DRX600 spectrometer equipped with a cryoprobe. The sample was exchanged for NMR into the following buffer: 25 mM Tris (pH 7.5)/50 mM NaCl/1 mM EDTA/1 mM DTT in 90% H₂O and 10% D₂O. The following parameters were used in the 3-D experiments: for HNCA, data size=2048 (t3)×32 (t2)×88 (t1) complex points, number of scans=16; for HN(CO)CA, data size=2048 (t3)×32 (t2)×88 (t1) complex points, number of scans=24. The delay time between each scan is 1.5 s.

For the complex between triply labeled [^2H , ^{13}C , ^{15}N] I κ B α (67–287) and [^2H]-p50(248–350)/p65(190–321), NMR spectra were acquired at 25 °C using TROSY-type triple-resonance experiments.³² To avoid the effects of fast transverse ^{13}C relaxation due to chemical shift anisotropy at high magnetic field, the TROSY-HN(CO)CA, TROSY-HN(COCA)CB and HNCO were acquired on a Bruker DRX600 spectrometer, whereas the TROSY-HNCA and TROSY-HN(CA)CB were acquired on a Bruker Avance900 spectrometer. The sample was exchanged for NMR into the following buffer: 25 mM D-Tris (pH 7.5)/50 mM NaCl/1 mM EDTA/1 mM DTT in 90% H $_2$ O and 10% D $_2$ O. The following parameters were used in the 3-D TROSY-based experiments: for TROSY-HNCA, data size=2048 (t $_3$) \times 64 (t $_2$) \times 96 (t $_1$) complex points, number of scans=32; for TROSY-HN(CO)CA, data size=1024 (t $_3$) \times 58 (t $_2$) \times 96 (t $_1$) complex points, number of scans=32; for TROSY-HN(CA)CB, data size=2048 (t $_3$) \times 56 (t $_2$) \times 96 (t $_1$) complex points, number of scans=64; for TROSY-HN(COCA)CB, data size=1024 (t $_3$) \times 56 (t $_2$) \times 96 (t $_1$) complex points, number of scans=48; for TROSY-HNCO, data size=1024 (t $_3$) \times 64 (t $_2$) \times 80 (t $_1$) complex points, number of scans=16. The delay time between each scan is 1.25 s.

For the complex between triply labeled [^2H , ^{13}C , ^{15}N] I κ B α (67–287) and [^2H]-p50(248–350)/p65(190–321), a TROSY-type HNCA spectrum was acquired at 30 °C on a Bruker Avance900 spectrometer. The sample was exchanged for NMR into the following buffer: 25 mM D-Tris (pH 7.5)/50 mM NaCl/1 mM EDTA/1 mM DTT in 90% H $_2$ O and 10% D $_2$ O. The parameters used in the TROSY-HNCA are data size=2048 (t $_3$) \times 64 (t $_2$) \times 96 (t $_1$) complex points, number of scans=32 and delay time between each scan=1.25 s.

NMR relaxation measurements

Measurements of T_1 and T_2 relaxation times and the ^1H - ^{15}N heteronuclear NOE for free I κ B α were made at 20 °C with uniformly [^{15}N , ^2H]-labeled I κ B α (67–206), and for bound I κ B α at 30 °C with uniformly ^{15}N , ^2H -labeled I κ B α (67–287) in complex with ^2H -labeled p50(248–350)/p65(190–321). T_1 and T_2 relaxation measurements were obtained on a Bruker DRX600 using published pulse programs.⁴⁹ For I κ B α (67–206), T_1 delays of 12, 177, 353, 705, 1057, 1409, 1761, 2201 and 2817 ms were used, with 12, 1057 and 2817 ms repeated; T_2 delays of 9, 13, 21, 37, 53, 69, 85, 101 and 117 ms were used, with 9, 53 and 117 ms repeated. For the I κ B α (67–287)/p50(248–350)/p65(190–321) complex, T_1 delays of 12, 45, 89, 177, 353, 705, 1057, 1409 and 2201 ms were used, with 12, 705 and 2201 ms repeated; T_2 delays of 9, 13, 17, 21, 29, 37, 53 and 61 ms were used, with 9, 29 and 61 ms repeated. For the ^1H - ^{15}N NOE measurements, independent saturated and unsaturated spectra were recorded in an interleaved manner for each sample. Data were processed using NMRpipe⁵⁰ and analyzed using NMRView⁵¹ and the program Curvfit.⁵²

H/D exchange experiments

Measurements of H/D exchange for free I κ B α were made at 20 °C with uniformly ^{15}N , ^2H -labeled I κ B α (67–206), and for bound I κ B α at 25 °C with uniformly ^{15}N , ^2H -labeled I κ B α (67–287) in complex with ^2H -labeled p50(248–350)/p65(190–321). H/D exchange was initiated by rapid buffer exchange from H $_2$ O into 100% D $_2$ O (pD 7.1), using a spin column. A series of ^1H - ^{15}N HSQC spectra⁵³ [free I κ B α (67–206)] or ^1H - ^{15}N TROSY-HSQC spectra⁵⁴ [I κ B α (67–287)/p50(248–350)/p65(190–321) complex] were acquired every 30 min on Bruker DRX600 or Avance900 spectrometers,

respectively, during a total exchange time of 30 h. The first experiments were started within 15 min after buffer exchange. Protection factors were determined by calculating $k_{\text{int}}/k_{\text{ex}}$, where k_{ex} is the exchange rate constant obtained by fitting a single-exponential function to the intensities of amides in the series of HSQCs and k_{int} is the intrinsic exchange rate constant obtained by using the program SPHERE†, which corrects for pH and temperature effects.³⁷ To obtain an estimate of the standard errors, each exchange experiment was repeated twice.

Supplementary Data

Supplementary data associated with this article can be found, in the online version, at [doi:10.1016/j.jmb.2008.05.048](https://doi.org/10.1016/j.jmb.2008.05.048)

References

- Baeuerle, P. A. & Baltimore, D. (1996). NF- κ B: ten years after. *Cell*, **87**, 13–20.
- Pahl, H. L. (1999). Activators and target genes of Rel/NF- κ B transcription factors. *Oncogene*, **18**, 6853–6866.
- Hoffmann, A., Natoli, G. & Ghosh, G. (2006). Transcriptional regulation via the NF- κ B signaling module. *Oncogene*, **25**, 6706–6716.
- Gilmore, T. D. (2006). Introduction to NF- κ B: players, pathways, perspectives. *Oncogene*, **25**, 6680–6684.
- Sen, R. & Baltimore, D. (1986). Inducibility of κ immunoglobulin enhancer-binding protein NF- κ B by a posttranslational mechanism. *Cell*, **47**, 921–928.
- Baldwin, A. S. (1996). The NF- κ B and I- κ B proteins: new discoveries and insights. *Annu. Rev. Immunol.* **14**, 649–683.
- Malek, S., Huxford, T. & Ghosh, G. (1998). I κ B α functions through direct contacts with the nuclear localization signals and the DNA binding sequences of NF- κ B. *J. Biol. Chem.* **273**, 25427–25435.
- Baeuerle, P. A. (1998). I κ B–NF- κ B structures: at the interface of inflammation control. *Cell*, **95**, 729–731.
- Huxford, T., Huang, D. B., Malek, S. & Ghosh, G. (1998). The crystal structure of the I κ B α /NF- κ B complex reveals mechanisms of NF- κ B inactivation. *Cell*, **95**, 759–770.
- Jacobs, M. D. & Harrison, S. C. (1998). Structure of an I κ B α /NF- κ B complex. *Cell*, **95**, 749–758.
- Malek, S., Huang, D. B., Huxford, T., Ghosh, S. & Ghosh, G. (2003). X-ray crystal structure of an I κ B β \times NF- κ B p65 homodimer complex. *J. Biol. Chem.* **278**, 23094–23100.
- Malek, S., Chen, Y., Huxford, T. & Ghosh, G. (2001). I κ B β , but not I κ B α , functions as a classical cytoplasmic inhibitor of NF- κ B dimers by masking both NF- κ B nuclear localization sequences in resting cells. *J. Biol. Chem.* **276**, 45225–45235.
- Huang, T. T., Kudo, N., Yoshida, M. & Miyamoto, S. (2000). A nuclear export signal in the N-terminal regulatory domain of I κ B α controls cytoplasmic localization of inactive NF- κ B/I κ B α complexes. *Proc. Natl Acad. Sci. USA*, **97**, 1014–1019.
- Harhaj, E. W. & Sun, S. C. (1999). Regulation of RelA subcellular localization by a putative nuclear export signal and p50. *Mol. Cell Biol.* **19**, 7088–7095.
- Hayden, M. S. & Ghosh, S. (2004). Signaling to NF- κ B. *Genes Dev.* **18**, 2195–2224.
- Mosavi, L. K., Cammett, T. J., Desrosiers, D. C. & Peng,

† www.fccc.edu/research/labs/roder/sphere/sphere.html

- Z. Y. (2004). The ankyrin repeat as molecular architecture for protein recognition. *Protein Sci.* **13**, 1435–1448.
17. Rechsteiner, M. & Rogers, S. W. (1996). PEST sequences and regulation by proteolysis. *Trends Biochem. Sci.* **21**, 267–271.
 18. Rogers, S., Wells, R. & Rechsteiner, M. (1986). Amino acid sequences common to rapidly degraded proteins: the PEST hypothesis. *Science*, **234**, 364–368.
 19. Croy, C. H., Bergqvist, S., Huxford, T., Ghosh, G. & Komives, E. A. (2004). Biophysical characterization of the free I κ B α ankyrin repeat domain in solution. *Protein Sci.* **13**, 1767–1777.
 20. Bergqvist, S., Croy, C. H., Kjaergaard, M., Huxford, T., Ghosh, G. & Komives, E. A. (2006). Thermodynamics reveal that helix four in the NLS of NF- κ B p65 anchors I κ B α , forming a very stable complex. *J. Mol. Biol.* **360**, 421–434.
 21. Truhlar, S. M., Torpey, J. W. & Komives, E. A. (2006). Regions of I κ B α that are critical for its inhibition of NF- κ B-DNA interaction fold upon binding to NF- κ B. *Proc. Natl. Acad. Sci. USA*, **103**, 18951–18956.
 22. Wright, P. E. & Dyson, H. J. (1999). Intrinsically unstructured proteins: Re-assessing the protein structure-function paradigm. *J. Mol. Biol.* **293**, 321–331.
 23. Iakoucheva, L. M., Brown, C. J., Lawson, J. D., Obradovic, Z. & Dunker, A. K. (2002). Intrinsic disorder in cell-signaling and cancer-associated proteins. *J. Mol. Biol.* **323**, 573–584.
 24. Liu, J., Perumal, N. B., Oldfield, C. J., Su, E. W., Uversky, V. N. & Dunker, A. K. (2006). Intrinsic disorder in transcription factors. *Biochemistry*, **45**, 6873–6888.
 25. Dyson, H. J. & Wright, P. E. (2005). Intrinsically unstructured proteins and their functions. *Nat. Rev. Mol. Cell Biol.* **6**, 197–208.
 26. Phelps, C. B., Sengchanthalangsy, L. L., Huxford, T. & Ghosh, G. (2000). Mechanism of I κ B α binding to NF- κ B dimers. *J. Biol. Chem.* **275**, 29840–29846.
 27. Mathes, E., O'Dea, E., Hoffmann, A. & Ghosh, G. (2008). NF- κ B dictates I κ B degradation modes. *EMBO J.* **27**, 1357–1367.
 28. Fiaux, J., Bertelsen, E. B., Horwich, A. L. & Wüthrich, K. (2002). NMR analysis of a 900 K GroEL-GroES complex. *Nature*, **418**, 207–211.
 29. Sprangers, R. & Kay, L. E. (2007). Quantitative dynamics and binding studies of the 20S proteasome by NMR. *Nature*, **445**, 618–622.
 30. Chen, F. E., Huang, D. B., Chen, Y. Q. & Ghosh, G. (1998). Crystal structure of p50/p65 heterodimer of transcription factor NF- κ B bound to DNA. *Nature*, **391**, 410–413.
 31. Yamazaki, T., Lee, W., Arrowsmith, C. H., Muhandiram, D. R. & Kay, L. E. (1994). A suite of triple-resonance NMR experiments for the backbone assignment of ^{15}N , ^{13}C , ^2H labeled proteins with high sensitivity. *J. Am. Chem. Soc.* **116**, 11655–11666.
 32. Salzmann, M., Wider, G., Pervushin, K., Senn, H. & Wüthrich, K. (1999). TROSY-type triple-resonance experiments for sequential NMR assignments of large proteins. *J. Am. Chem. Soc.* **121**, 844–848.
 33. Schwarzingger, S., Kroon, G. J. A., Foss, T. R., Chung, J., Wright, P. E. & Dyson, H. J. (2001). Sequence dependent correction of random coil NMR chemical shifts. *J. Am. Chem. Soc.* **123**, 2970–2978.
 34. Metzler, W. J., Constantine, K. L., Friedrichs, M. S., Bell, A. J., Ernst, E. G., Lavoie, T. B. & Mueller, L. (1993). Characterization of the three-dimensional solution structure of human profilin: ^1H , ^{13}C , and ^{15}N NMR assignments and global folding pattern. *Biochemistry*, **32**, 13818–13829.
 35. Gardner, K. H., Rosen, M. K. & Kay, L. E. (1997). Global folds of highly deuterated, methyl-protonated proteins by multidimensional NMR. *Biochemistry*, **36**, 1389–1401.
 36. Englander, S. W. (1980). Internal motions in proteins and nucleic acids and their hydrogen exchange properties.; [Comments]. *Mol. Cell Biophys.* **1**, 15–28.
 37. Bai, Y., Milne, J. S., Mayne, L. & Englander, S. W. (1993). Primary structure effects on peptide group hydrogen exchange. *Proteins*, **17**, 75–86.
 38. Clarke, J. & Itzhaki, L. S. (1998). Hydrogen exchange and protein folding. *Curr. Opin. Struct. Biol.* **8**, 112–118.
 39. Ferreira, D. U., Cervantes, C. F., Truhlar, S. M., Cho, S. S., Wolynes, P. G. & Komives, E. A. (2007). Stabilizing I κ B α by “consensus” design. *J. Mol. Biol.* **365**, 1201–1216.
 40. Linderström-Lang, K. (1955). Deuterium exchange between peptides and water. *Chem. Soc. Spec. Publ.* **2**, 1–20.
 41. Eliezer, D. & Wright, P. E. (1996). Is apomyoglobin a molten globule? Structural characterization by NMR. *J. Mol. Biol.* **263**, 531–538.
 42. Hilser, V. J. & Thompson, E. B. (2007). Intrinsic disorder as a mechanism to optimize allosteric coupling in proteins. *Proc. Natl. Acad. Sci. USA*, **104**, 8311–8315.
 43. Truhlar, S. M., Mathes, E., Cervantes, C. F., Ghosh, G. & Komives, E. A. (2008). Pre-folding I κ B α alters control of NF- κ B signaling. *J. Mol. Biol.* In press. doi: 10.1016/j.jmb.2008.02.053.
 44. Gunasekaran, K., Tsai, C. J., Kumar, S., Zanuy, D. & Nussinov, R. (2003). Extended disordered proteins: targeting function with less scaffold. *Trends Biochem. Sci.* **28**, 81–85.
 45. Huxford, T., Mishler, D., Phelps, C. B., Huang, D. B., Sengchanthalangsy, L. L., Reeves, R. et al. (2002). Solvent exposed non-contacting amino acids play a critical role in NF- κ B/I κ B α complex formation. *J. Mol. Biol.* **324**, 587–597.
 46. Chen, F. E., Kempiak, S., Huang, D. B., Phelps, C. & Ghosh, G. (1999). Construction, expression, purification and functional analysis of recombinant NF κ B p50/p65 heterodimer. *Protein Eng.* **12**, 423–428.
 47. Grzesiek, S. & Bax, A. (1992). Improved 3D triple-resonance NMR techniques applied to a 31 kDa protein. *J. Magn. Reson.* **96**, 432–440.
 48. Wittekind, M. & Mueller, L. (1993). HNCACB, a high-sensitivity 3D NMR experiment to correlate amide-proton and nitrogen resonances with the alpha- and beta-carbon resonances in proteins. *J. Magn. Reson.* **101**, 201–205.
 49. Farrow, N. A., Muhandiram, R., Singer, A. U., Pascal, S. M., Kay, C. M., Gish, G. et al. (1994). Backbone dynamics of a free and a phosphopeptide-complexed Src homology 2 domain studied by ^{15}N NMR relaxation. *Biochemistry*, **33**, 5984–6003.
 50. Delaglio, F., Grzesiek, S., Vuister, G. W., Guang, Z., Pfeifer, J. & Bax, A. (1995). NMRPipe: a multidimensional spectral processing system based on UNIX pipes. *J. Biomol. NMR*, **6**, 277–293.
 51. Johnson, B. A. & Blevins, R. A. (1994). NMRView: a computer program for the visualization and analysis of NMR data. *J. Biomol. NMR*, **4**, 604–613.
 52. Mandel, A. M., Akke, M. & Palmer, A. G. (1995). Backbone dynamics of *Escherichia coli* ribonuclease HI: correlations with structure and function in an active enzyme. *J. Mol. Biol.* **246**, 144–163.
 53. Grzesiek, S. & Bax, A. (1993). The importance of not saturating H $_2$ O in protein NMR. Application to sensitivity enhancement and NOE measurements. *J. Am. Chem. Soc.* **115**, 12593–12594.
 54. Schulte-Herbruggen, T. & Sørensen, O. W. (2000). Clean TROSY: compensation for relaxation-induced artifacts. *J. Magn. Reson.* **144**, 123–128.